



RESEARCH ARTICLE

10.1002/2016EA000187

Key Points:

- First successful air-deployed launch of an unmanned aircraft system into a mature hurricane
- Data collected from the Coyote unmanned aircraft compared favorably with conventional observations collected from NOAA's P-3 aircraft

Correspondence to:

J. J. Cione,
joe.cione@noaa.gov

Citation:

Cione, J. J., E. A. Kalina, E. W. Uhlhorn, A. M. Farber, and B. Damiano (2016), Coyote unmanned aircraft system observations in Hurricane Edouard (2014), *Earth and Space Science*, 3, 370–380, doi:10.1002/2016EA000187.

Received 31 MAY 2016

Accepted 30 AUG 2016

Accepted article online 8 SEP 2016

Published online 30 SEP 2016

Coyote unmanned aircraft system observations in Hurricane Edouard (2014)

J. J. Cione^{1,2}, E. A. Kalina^{1,2}, E. W. Uhlhorn³, A. M. Farber⁴, and B. Damiano⁵

¹Hurricane Research Division, NOAA's Atlantic Oceanographic and Meteorological Laboratory, Miami, Florida, USA,

²Physical Sciences Division, NOAA's Earth System Research Laboratory, Boulder, Colorado, USA, ³Physical Sciences

AIR-Worldwide, Boston, Massachusetts, USA, ⁴Raytheon Missile Systems, Tucson, Arizona, USA, ⁵Data and Development Section, NOAA's Aircraft Operations Center, MacDill Air Force Base, Tampa, Florida, USA

Abstract Horizontal wind, temperature, and moisture observations are presented from two Coyote unmanned aircraft system (UAS) flights in the boundary layer of Hurricane Edouard (2014). The first flight sampled the meteorological conditions in the eye and eyewall at altitudes from 900 to 1500 m while Edouard was a major hurricane (105 kt) on 16 September 2014. The following day, a second Coyote sampled the inflow layer outside of the storm core at ~760 m altitude, when Edouard had weakened to an 80-kt hurricane. These flights represent the first deployments of a UAS from an airborne manned aircraft into a tropical cyclone. Comparisons between the Coyote data and the Lockheed WP-3D Orion (WP-3D) flight-level measurements and analyses constructed from dropsonde data are also provided. On 16 September 2014, the Coyote-measured horizontal wind speeds agree, on average, to within $\sim 1 \text{ m s}^{-1}$ of the wind speeds observed by the WP-3D and reproduce the shape of the radial wind profile from the WP-3D measurements. For the inflow layer experiment on 17 September, the mean wind speeds from the Coyote and the dropsonde analysis differ by only 0.5 m s^{-1} , while the Coyote captured increased variability ($\sigma = 3.4 \text{ m s}^{-1}$) in the horizontal wind field compared to the dropsonde analysis ($\sigma = 2.2 \text{ m s}^{-1}$). Thermodynamic data from the Coyote and dropsondes agree well for both flights, with average discrepancies of 0.4°C and 0.0°C for temperature and 0.7°C and 1.3°C for dew point temperature on 16 and 17 September, respectively

1. Introduction

The open-ocean tropical cyclone (TC) boundary layer requires intensive scientific observation because it controls the exchanges of heat, moisture, and momentum that ultimately modulate TC intensity. However, low-altitude ($z < 1 \text{ km}$) measurements of the TC boundary layer by manned aircraft are rare and exceptionally dangerous due to the hazards posed by large waves, convective downdrafts, and sea spray. Save for a few notable exceptions [Black *et al.*, 2007; Zhang *et al.*, 2008], hurricane reconnaissance aircraft, such as the Lockheed WP-3D Orion, do not typically descend below $\sim 3 \text{ km}$ in hurricanes. As a result, the only data that are routinely collected in the TC boundary layer are (1) limited point thermodynamic and kinematic measurements made by dropsondes [Hock and Franklin, 1999] and ocean buoys [Cione *et al.*, 2000; Cione *et al.*, 2013], and (2) remote kinematic measurements by airborne radar [Jorgensen, 1984] and stepped frequency microwave radiometry [Uhlhorn and Black, 2003; Uhlhorn *et al.*, 2007]. The deployment of an unmanned aircraft system (UAS) within the TC boundary layer therefore has the potential to address the critical data gaps that currently exist in this understudied region. To this end, two Coyote UASs were launched into Hurricane Edouard (2014) and collected low-altitude thermodynamic and kinematic measurements in the eye, eyewall, and inflow layer of the hurricane from 16 to 17 September 2014. These missions mark the first time a UAS was deployed into a TC using a manned aircraft as the delivery vehicle. A primary goal of this research will be to compare Coyote UAS observations with other known measurement platforms and sensors in Hurricane Edouard using NOAA's WP-3D aircraft.

Prior to the Coyote deployments in Hurricane Edouard (2014), only three UAS flights had been conducted in TCs: a 2005 flight into the inner core of Tropical Storm Ophelia at a height of $\sim 760 \text{ m}$ [Cione *et al.*, 2008; Cascella *et al.*, 2008], a 2005 flight that penetrated the eyewall of Typhoon Longwang at 3000 m [Lin and Lee, 2008], and a 2007 flight into the eyewall of Hurricane Noel at heights as low as $\sim 90 \text{ m}$ [Cascella *et al.*, 2008]. These landmark missions illustrate the potential of UASs to make measurements in the severe and varied conditions of the hurricane environment. However, all of the aforementioned studies were deployed

©2016. The Authors.

This is an open access article under the terms of the Creative Commons Attribution-NonCommercial-NoDerivs License, which permits use and distribution in any medium, provided the original work is properly cited, the use is non-commercial and no modifications or adaptations are made.

from land and did not utilize a manned aircraft for launch. In addition, the earlier cases did not compare UAS data with measurements from any other observing platforms. As such, the accuracy of UAS measurements in TCs remains unknown.

In this paper, we take the data obtained from the two Coyote UAS flights in Hurricane Edouard and compare them with more conventional data sources, which include dropsondes and the WP-3D flight-level wind measurements. Specifically, comparisons for air temperature, dew point temperature, and wind speed measured by UAS during the two missions are presented. We begin by providing an overview of the life cycle of Hurricane Edouard and the Coyote UAS missions in section 2. Section 3 describes the methods used to create the analyses that are compared against the Coyote data presented in section 4. Results are summarized and concluding remarks are provided in section 5.

2. Coyote UAS Operations in Hurricane Edouard

2.1. Hurricane Edouard

The area of low pressure that eventually became Edouard formed from a tropical wave that exited the coast of western Africa in the Intertropical Convergence Zone. The National Hurricane Center issued the first advisory on the storm at 1500 UTC on 11 September 2014. Over the next 2 days, the system gradually became more organized as it moved northwestward over the open tropical Atlantic. Edouard attained tropical storm status at 0000 UTC on 12 September and hurricane status at 1200 UTC on 14 September. The hurricane continued to intensify steadily, and its maximum sustained winds reached an estimated peak speed of 105 kt ($\sim 54 \text{ m s}^{-1}$) at 1200 UTC on 16 September. Thereafter, Edouard encountered increasing vertical wind shear and cooler ocean temperatures as it accelerated to the north. The storm underwent a gradual weakening trend, losing hurricane status on 18 September and weakening to a remnant low on the following day. Further information on the life cycle of Hurricane Edouard can be found in *Stewart* [2014].

Edouard posed no serious threat to land areas during its 9-day lifetime. The storm passed ~ 1300 km to the east of Bermuda at its closest approach on 16 September. Because the island experienced no direct impacts from Edouard but was within aircraft reconnaissance range of the storm from 15 to 17 September, Bermuda served as an ideal location to conduct research missions into the hurricane. In the next section, we summarize the operations related to the Coyote deployments.

2.2. Description of the Coyote UAS and Hurricane Edouard Deployments

Manufactured by Raytheon Missile Systems, Coyote has a length of 0.79 m, a wingspan of 1.47 m, and a mass of 6 kg. It is capable of carrying a payload of up to 1.8 kg. Its maximum cruising airspeed is $\sim 36 \text{ m s}^{-1}$. To facilitate deployments from the WP-3D, the wings of the Coyote are folded and the Coyote is placed inside a canister that is subsequently released from the sonobuoy chute aboard the WP-3D. Once deployed, a parachute slows the descent of the canister. After ~ 15 s (enough time for the turbulent motion of the canister to stabilize), the Coyote releases the canister, the Coyote's wings deploy and the UAS begins sampling the environment. The flight path, altitude, and airspeed are controlled by commands issued remotely from the WP-3D. In 2014, data were transmitted in real time back to the WP-3D using (1) an Iridium satellite connection and (2) a 900-MHz data stream.

Two Coyote deployments were conducted in Hurricane Edouard. The first Coyote was released at a height of ~ 3 km from NOAA's WP-3D into the eye of Hurricane Edouard on 16 September at 1433 UTC. This marked the first time that a UAS was air deployed into a hurricane and the first ever Coyote hurricane flight. Following its release, Coyote collected data in the eye and, later, in the western eyewall of Edouard for ~ 27 min while the storm was at its estimated peak intensity of 105 kt ($\sim 54 \text{ m s}^{-1}$; Table 1). Limited data ($\sim 7\%$ of the total number of 1-s samples) were retrieved from the eyewall because the Iridium satellite connection proved to be unreliable, and the 900-MHz data stream required the WP-3D to remain within 8–11 km range of the Coyote.

The second Coyote deployment occurred the following day at 1508 UTC on 17 September. Unlike the previous mission, the second Coyote was air deployed ~ 280 km from the storm center to collect low-altitude (~ 760 m) kinematic and thermodynamic data in the hurricane inflow layer (Table 1). The Coyote flew for ~ 68 min (a platform endurance record) before exhausting its onboard battery and ditching into the ocean

Table 1. Coyote Missions in Hurricane Edouard

Date	Coyote Flight Times (UTC)	Locations and Heights Targeted	Hurricane Intensity Wind (kt)/Pressure (hPa)
16 September 2014	1433–1500(27 min)	Eye and eyewall(900–1500 m)	105/955
17 September 2014	1508–1616(68 min)	Clear air and rainband in inflow layer (~760 m)	80/957

~150 km from the storm center. Based on lessons learned from the previous day, the WP-3D remained within ~6 km range of the Coyote, allowing for more continuous data to be collected.

2.3. Coyote Measurements

Both of the Coyotes were equipped with meteorological sensors that measured temperature, relative humidity, and atmospheric pressure. Table 2 provides details on each of the meteorological sensors. According to the manufacturer, the maximum expected errors for the temperature and humidity sensors were ±0.3°C and ±5%, respectively, while the sampling rates were 2 Hz and 1 Hz, respectively. At a speed of 40 m s⁻¹ (representative of the Coyote ground speed during these missions), these sampling rates resulted in a temperature (humidity) measurement for every 20 m (40 m) of horizontal distance traveled.

Instantaneous wind speed and direction (also reported at 1 Hz) are computed by vector subtraction of the true air velocity from the ground velocity. The ground velocity vector is computed via a 50-Hz GPS/INS extended Kalman filter implemented within the autopilot. Inputs to the filter are IMU, air data and GPS position, and velocity. To determine the true air velocity vector, the equivalent airspeed (EAS) is first calculated using $EAS = \sqrt{2Q/\rho_0}$, where ρ_0 is the air density at mean sea level pressure, equal to 1.225 kg m⁻³, and Q is the dynamic pressure (Pa; the air pressure induced by the wind-relative motion of the Coyote). The dynamic pressure is the difference between the pitot pressure and the static pressure, both of which are measured directly by onboard sensors. EAS is assumed to be equal to indicated airspeed, because air compressibility is negligible at the relatively slow speeds (~28 m s⁻¹) flown by the Coyote. The magnitude of the true air speed (TAS) vector is then computed from $TAS = IAS\sqrt{\rho_0/\rho}$, where ρ is the local air density (kg m⁻³). The direction of the TAS vector is also an output of the Kalman filter, as it requires deriving the Euler angles of the vehicle using all of the autopilot’s onboard sensor data (IMU, air data and GPS). The details of this Kalman filter are proprietary and are therefore not available for publication. However, future advances to the Coyote platform should allow for more customized tuning of this filter to provide a deeper and more confident understanding of how these values are computed.

It is important to note that the sensor accuracies and response times listed in Table 2 were determined in a laboratory setting, not in the strong winds, turbulence, and heavy rainfall characteristic of a tropical cyclone. In such an environment, the sensors might not perform as indicated in Table 2. Thus, an extensive portion of this manuscript is devoted to comparing the Coyote measurements to other data sets, including dropsonde data and flight-level wind measurements, to estimate the Coyote data accuracy.

3. Comparison Method

3.1. GPS Dropsonde Data

GPS dropsonde measurements of temperature, dew point temperature, radial wind, and total wind formed the basis for comparison to the Coyote data, except for the WP-3D flight-level wind measurements used in the wind speed comparison on 16 September 2014 (described in section 3.2). Figure 1 shows the drop-to-splash paths of the dropsonde data relative to the Coyote track. For each of the relevant variables, the dropsonde data were used to construct an analysis that could then be compared to the Coyote measurements. For the eye/eyewall mission on 16 September, dropsonde observations from two WP-3D flights (N42RF: 1357–1800

Table 2. Specifications for the Meteorological Sensors Aboard the Coyote

Sensor	Manufacturer Model	Range	Tolerance	Response Time (s)	Sampling Rate (Hz)
Pressure	HoneywellSCCP15ASMTP	5–1070 mb	±0.5 mb	<1.0	3
Temperature	SHIBAURAPB5	–80–60°C	±0.3°C	<2.0	2
Humidity	E + EHC103M2	0–100%	±5%	<5.0 at 25°C	1

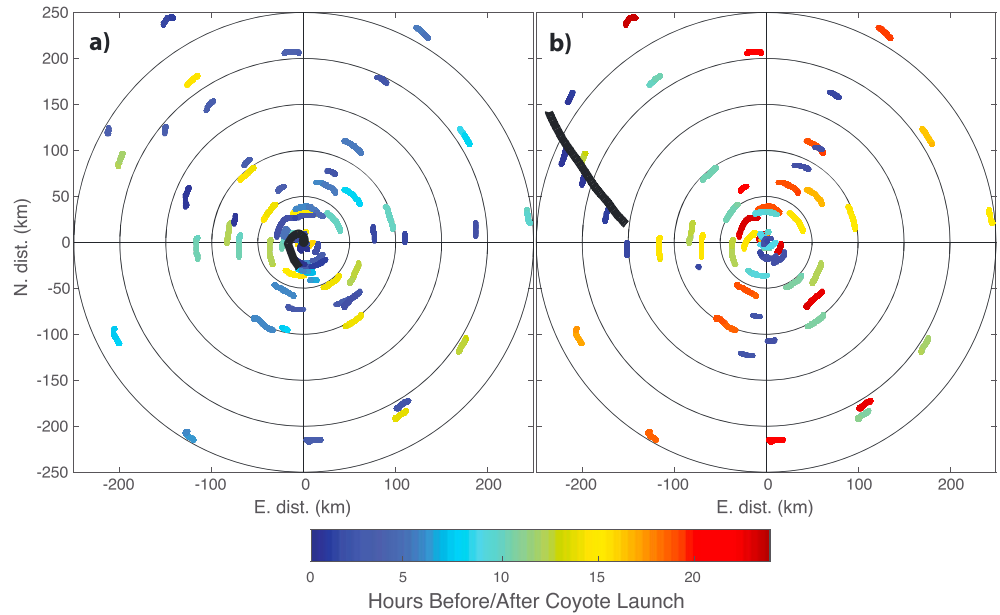


Figure 1. Dropsonde tracks, from launch to splash, included in the analyses on (a) 16 September 2014 and (b) 17 September 2014. The colors indicate the amount of time that elapsed between the Coyote and dropsonde launches. The Coyote tracks are shown in black.

UTC and N43RF: 1903–2202 UTC) and a Global Hawk mission (16 September 2014 1506 UTC to 17 September 2014 0828 UTC) were used to construct the analysis. For the inflow layer mission on the following day, dropsonde observations from one WP-3D flight (N42RF: 1258–1653 UTC) and the Global Hawk mission (16 September 2014 1506 UTC to 17 September 2014 0828 UTC) were considered.

Dropsonde measurements were interpolated to the Coyote flight track in storm-centered, storm-relative radius, azimuth, and altitude as functions of time $[r(t), \lambda(t), z(t)]$ using a weighted average of surrounding observations. The weights were assumed to be Gaussian and nonisotropic, that is

$$w_i = \exp(-d_i), \tag{1}$$

where d_i is the sum of squared normalized distances in space and time from a grid point to the i th observation:

$$d_i = \ln(2) \left[\left(\frac{\Delta r}{s_r} \right)^2 + \left(\frac{\Delta \lambda}{s_\lambda} \right)^2 + \left(\frac{\Delta z}{s_z} \right)^2 + \left(\frac{\Delta t}{s_t} \right)^2 \right]. \tag{2}$$

The factor $\ln(2)$ ensures that the weight decreases to 0.5 at the specified scale distance. The analysis value (Y_a) at the flight track grid point was then computed from the observations (y) as

$$Y_a = \frac{\sum_i w_i y_i}{\sum_i w_i}. \tag{3}$$

The scaling parameters (s) were chosen empirically depending on whether the analysis was for the eyewall or inflow layer experiments. For the eyewall, the storm structure was assumed to be more azimuthally symmetric with large gradients in the radial direction, and so we chose $s_r = 5$ km and $s_\lambda = 45^\circ$. Conversely, well outside the eyewall for the inflow analysis, we assumed radial gradients to be smaller and set $s_r = 10$ km and $s_\lambda = 10^\circ$. For both the eyewall and inflow experiment analyses, $s_z = 100$ m and $s_t = 1$ h.

3.2. WP-3D Flight-Level Measurements

For the eye/eyewall mission on 16 September 2014 (section 4.1), the large wind speed gradient in the transition region between the eye and the eyewall precluded using the wind speed from the dropsonde analysis

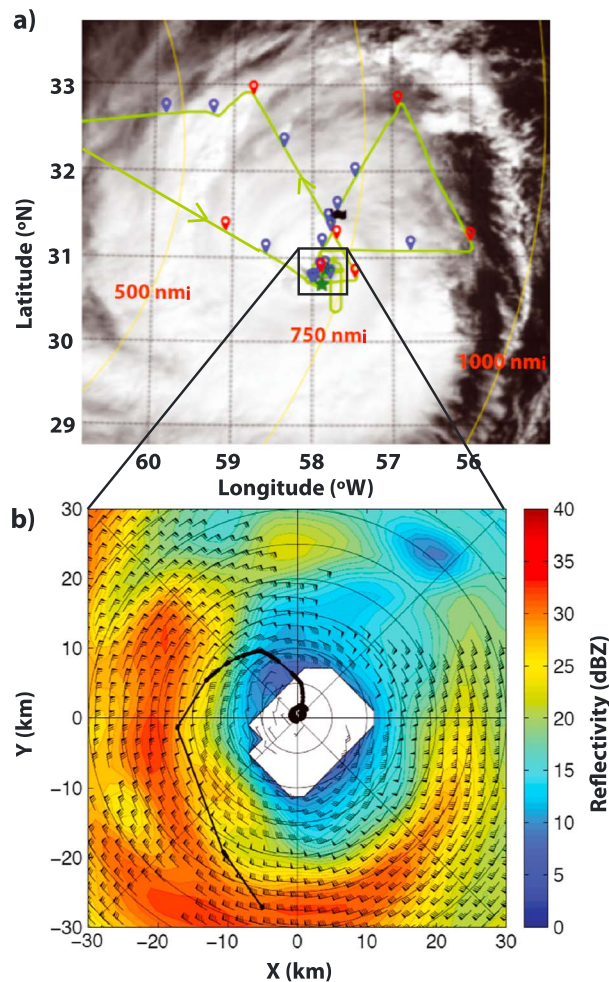


Figure 2. An overview of the Coyote eye/eyewall mission on 16 September 2014, showing (a) a visible satellite image of Hurricane Edouard taken by the Terra Moderate Resolution Imaging Spectroradiometer (MODIS) at 1420 UTC and (b) equivalent radar reflectivity (color fill; dBZ_e) and retrieved horizontal winds (barbs; knots) at z = 1 km from the N43RF Tail Doppler Radar at 1720 UTC. The green line in Figure 2a is the flight track of N42RF, while blue and red pins indicate the launch locations of dropsondes and dropsonde + airborne expendable bathythermograph pairs, respectively. Black flags and green stars show the locations of TC center fixes and Coyote launch/splash points, respectively. Numbers and range rings indicate distances to L.F. Wade International Airport, the takeoff and landing location for N42RF. The black line in Figure 2b is the approximate Coyote flight track. Satellite image is courtesy of http://www.nrlmry.navy.mil/tc_pages/tc_home.html.

~10 min of the flight, the Coyote circled through the light-wind region of the eye (Figure 2b) and measured wind speeds of 2–8 m s⁻¹ (Figure 3b). The Coyote then moved northwest to slowly exit the eye and to sample the eye-eyewall transition region from 10 to 20 km. During this time, the measured wind speed increased markedly from 8 to 32 m s⁻¹ (Figure 3b). The Coyote then proceeded to enter the western eyewall of Edouard (Figure 2b), and at a radial distance of ~22 km, the Coyote recorded a wind speed of 51.5 m s⁻¹ (a platform record; Figure 3b).

Figure 3b presents a comparison between the Coyote-measured wind speed and the WP-3D flight-level (z ~ 3 km) 1-s wind speed data (section 3.2). The Coyote and the WP-3D wind measurements depict similar trends (Figure 3b), with a light-wind region (0–10 m s⁻¹) from 0 to 10 km, a region where the wind speed

for comparison purposes. Instead, we used the 1-s flight-level wind measurements made by the WP-3D during the inbound and outbound flight legs that were closest in time to the Coyote launch. These data were collected from 1358 to 1417 UTC (inbound flight leg; northwest eyewall) and from 1502 to 1525 UTC (outbound flight leg; southern eyewall), as seen in Figure 2a (green flight track). The Coyote flew from 1433 to 1500 UTC in a counterclockwise semicircle from northwest of the eye to the southern eyewall (Figure 2b). Due to the proximity of the Coyote to the TC center on this day, only the total horizontal wind speed was compared between the two platforms, since the magnitude and sign of the radial component were highly sensitive to the exact location used for the TC center at such close range.

4. Comparisons Between Coyote and Dropsonde/WP-3D Flight-Level Data

4.1. 16 September 2014 Eye/Eyewall Mission

From 1433 to 1500 UTC on 16 September 2014, the first Coyote mission into Hurricane Edouard was conducted (Figure 2). This 27-min flight collected meteorological data from the eye and eyewall regions of the TC at altitudes that gradually decreased from 1500 m to 900 m (Table 1 and Figure 3a). The Coyote-measured wind speed as a function of radial distance from the TC center is shown in Figure 3b. During the first

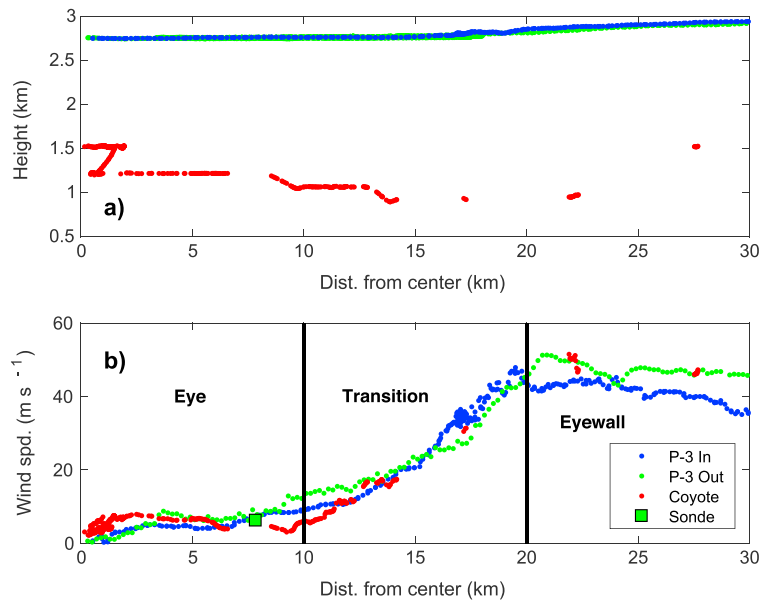


Figure 3. (a) Flight altitude and (b) wind speed measured with respect to radial distance for the Coyote (red) and the WP-3D inbound (blue) and outbound (green) legs during the 16 September 2014 mission. The green square indicates a measurement made by a dropsonde located 16 km from the Coyote (Table 4). The vertical black lines indicate the approximate boundaries between the eye, transition region, and eyewall.

increased from ~10 to 50 m s⁻¹ from radial distances of ~10 to 20 km and, finally, a region where the wind speed slowly decreased by ~5 m s⁻¹ beyond the eyewall from 20 to 30 km. The mean difference in wind speed between the Coyote and paired WP-3D measurements is 1.2 m s⁻¹ and 0.8 m s⁻¹ for the inbound and outbound WP-3D flight legs, respectively (Table 3). Also available for comparison was a dropsonde deployed within the southwest quadrant of the eye at a radial distance of 7.8 km (Table 4), which recorded a wind speed of 6.4 m s⁻¹ (green square in Figure 3b) at the Coyote’s altitude ($z = 1.06$ km). The dropsonde measurement suggests that the Coyote, which measured winds of ~5 m s⁻¹ between radial distances of 6 and 9 km in the northwest quadrant of the eye, reported realistic wind measurements there.

The peak winds measured by the Coyote and the WP-3D were 51.5 m s⁻¹ (Coyote), 47.9 m s⁻¹ (WP-3D inbound leg), and 51.3 m s⁻¹ (WP-3D outbound leg). In the eyewall, winds at the Coyote flight level ($z = 1$ km) are expected to be ~16% faster, on average, than winds at the WP-3D flight level ($z = 3$ km), based on an analysis of 429 eyewall vertical wind profiles collected by GPS dropsondes in 17 hurricanes [Franklin *et al.*, 2003]. If the WP-3D peak winds are increased by this amount, the values are 55.6 m s⁻¹ and 59.5 m s⁻¹. Although the peak wind speed measured by the Coyote was 4–8 m s⁻¹ slower than these estimates, communication issues between the WP-3D and the Coyote resulted in limited data retrieval from the eyewall, and it is therefore unlikely that the Coyote documented the peak wind that it encountered.

In addition to wind observations, the Coyote also measured air temperature (Figure 4a), relative humidity, and pressure. These measurements were used to calculate dew point temperature (Figure 4b), and the air and dew point temperatures were then compared to the dropsonde data analysis (section 3.1). Both the

Table 3. Comparison Between the Coyote Measurements and the Wind Speed From the WP-3D and the Temperature and Dew Point Temperature From the Dropsonde Analyses for the 16 September 2014 Eye/Eyewall Mission^a

Variable	Coyote	WP-3D Data or Dropsonde Analysis	Difference(Coyote-Analysis)
Wind speed (m s ⁻¹)	9.4 ± 11.0	8.2 ± 11.38.6 ± 12.1	1.2–0.3 (inbound leg) 0.8–1.1 (outbound leg)
Temperature (°C)	20.4 ± 0.8	20.0 ± 0.9	0.4 – 0.1
Dew point temperature (°C)	19.5 ± 1.2	18.8 ± 1.2	0.7 + 0.0

^aMeans (standard deviations) are listed to the left (right) of the ± symbols. Differences that are statistically significant at the 95% level are indicated in bold.

Table 4. Characteristics of the Dropsonde Data Shown in Figures 3, 4, 6, and 8 (Green Squares)^a

Dropsonde Launch Date/Time (UTC)	Coyote/Dropsonde Height (m)	Horizontal Distance Between Coyote/Dropsonde (km)
16 September 20141439	1060	16.1
17 September 20141529	750	18.4
17 September 20141543	760	8.08
17 September 20141605	460	18.5

^aThe horizontal distances between the dropsondes and the Coyote correspond to when the two platforms were at the same height.

Coyote measurements and the analysis reflect 2–3°C of warming (Figure 4a) as the Coyote gradually descended from 1500 m at the beginning of the flight to 900 m at $t = 15$ min (Figure 3a). This trend then reversed as the Coyote entered the western eyewall and climbed back to 1500 m. In a quantitative sense, 75% (46%) of the temperature data agree to within $\pm 1^\circ\text{C}$ (0.5°C). Discrepancies on the order of $\sim 1^\circ\text{C}$ are likely due to a combination of instrument noise and small-scale environmental variability measured by the Coyote, but not by the coarsely-spaced dropsondes. The mean difference between the two measurements is 0.4°C (Table 3). An individual temperature measurement made by a dropsonde in the southwest quadrant of the eye ~ 7.8 km from the center (Table 4; green square in Figure 4a) agrees well with the Coyote, as both platforms recorded a temperature of $\sim 21^\circ\text{C}$ at the same altitude. In regards to dew point temperature, there is slightly less agreement (Figure 4b), with 67% (40%) of the data within $\pm 1^\circ\text{C}$ (0.5°C), with a mean difference of 0.7°C . The data within the transition region (10–20 km), an area where moisture gradients are likely to be large, are mostly responsible for the increase in disagreement. Even within the transition region, however, the average discrepancy is $\sim 1^\circ\text{C}$.

4.2. 17 September 2014 Inflow Mission

From 1508 to 1616 UTC on 17 September 2014, a second Coyote was used to measure the air temperature, moisture, and winds in the inflow layer of Hurricane Edouard (Figure 5) at an altitude of ~ 760 m (Figure 6a). This 68-min flight documented the meteorological conditions between radial distances of 275 km and 150 km from the TC center in the northwestern quadrant of the storm. Figure 6 shows a comparison between the total wind speed (Figure 6b) and the radial wind speed component (Figure 6c) measured by Coyote and those obtained from an analysis of dropsonde wind measurements (section 3.1). The wind speeds obtained

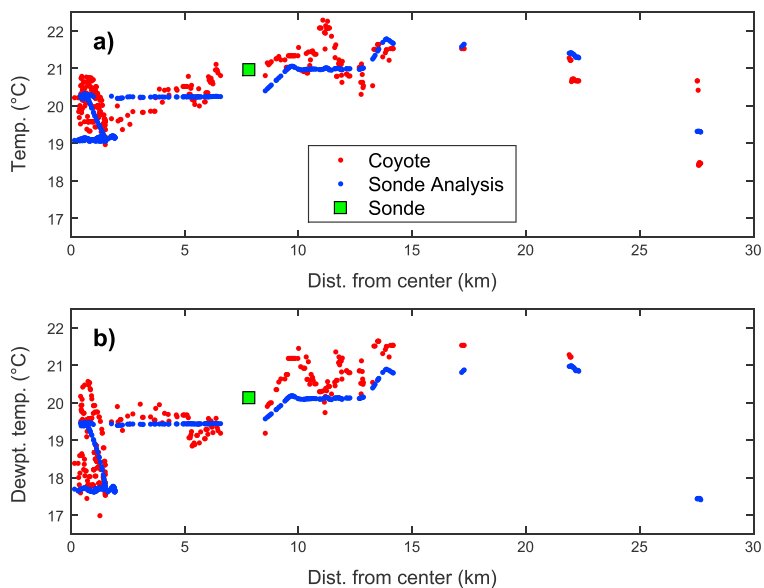


Figure 4. (a) Air temperature and (b) dew point temperature measured by Coyote (red) and from an analysis (blue) of dropsonde measurements for the 16 September 2014 Coyote flight. Green squares indicate measurements made by a dropsonde located 16 km from the Coyote (Table 4).

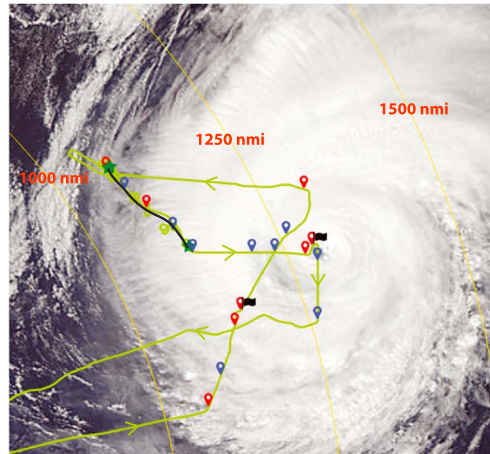


Figure 5. As in Figure 2a but for the Coyote inflow layer mission on 17 September 2014. The approximate Coyote flight track is shown in black. The visible satellite image was taken by Aqua MODIS at 1640 UTC. Satellite image is courtesy of NASA Goddard MODIS Rapid Response Team.

from the Coyote and the dropsonde wind analysis are in good agreement, with mean differences of 0.5 m s^{-1} (total wind; Figure 6b) and 0.8 m s^{-1} (radial wind; Figure 6c). Individual Coyote measurements that were nearly coincident in time and space with measurements made by three individual dropsondes (Table 4; green squares in Figure 6) also agree to within $\sim 2 \text{ m s}^{-1}$. These metrics suggest that the Coyote obtained wind measurements accurate to 2 m s^{-1} or better within the TC inflow layer. Figure 6 also suggests that the Coyote was able to measure the fine-scale structure and variability present within the wind field, which is difficult to accomplish using coarsely spaced GPS dropsondes.

This is reflected by comparing the standard deviations in the radial wind speeds measured by the Coyote (2.1 m s^{-1} ; Table 5) and from the dropsonde wind analysis (0.6 m s^{-1}). The former is 3.5 times larger, indicative of the increased variability in the wind field that can be detected with UAS platforms such as the Coyote.

The ability of the Coyote to finely sample the structure of the TC boundary layer allows for the identification of meteorological features that might otherwise be missed by more conventional measurement platforms. On 17 September, for instance, the Coyote sampled an outer rainband and its surrounding environment between 225 km and 190 km radial distance from the TC center. This rainband is apparent in imagery from the WP-3D lower fuselage (LF) radar (Figure 7), which measures radar reflectivity (but not Doppler velocity). The prerainband environment resulted in an increase in the Coyote-measured total wind speed from 18 m s^{-1} to 25 m s^{-1} (red points in Figure 6b from 225 to 190 km). This feature was not resolved by the

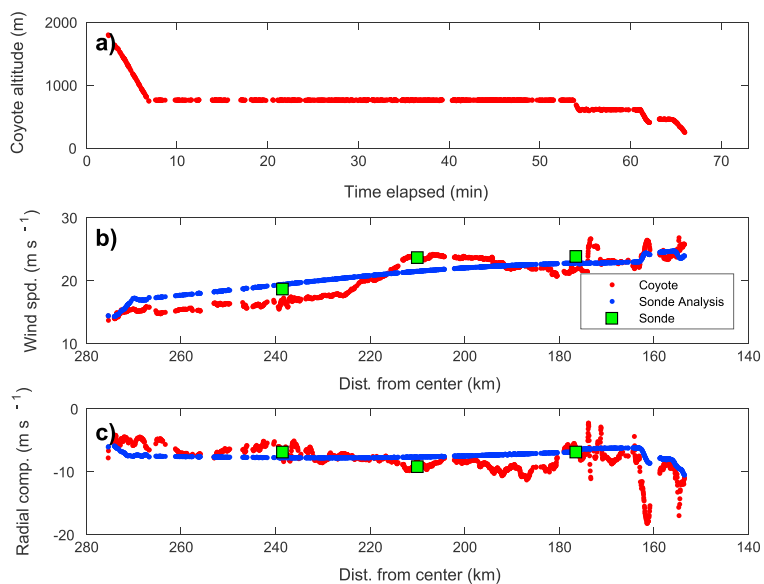


Figure 6. (a) Time series of Coyote altitude and comparison between (b) wind speed and (c) radial wind measured by Coyote (red) and from an analysis (blue) of dropsonde measurements for the 17 September 2014 mission. Green squares indicate measurements made by three dropsondes located within 20 km of the Coyote (Table 4).

Table 5. As in Table 3 but for the 17 September 2014 Inflow Layer Mission

Variable	Coyote	Analysis	Difference (Coyote-Analysis)
Wind speed (m s^{-1})	20.7 ± 3.4	21.2 ± 2.2	-0.5 ± 1.2
Radial wind speed (m s^{-1})	-8.2 ± 2.1	-7.4 ± 0.6	-0.8 ± 1.5
Temperature ($^{\circ}\text{C}$)	20.9 ± 1.0	20.9 ± 1.2	$0.0 - 0.2$
Dew point temperature ($^{\circ}\text{C}$)	19.8 ± 1.3	18.5 ± 1.6	$1.3 - 0.3$

dropsonde wind analysis (blue points in Figure 6b). Therefore, the Coyote was the only measurement platform that documented the full (i.e., kinematic and thermodynamic) boundary layer characteristics of the rainband and its environment on this day.

Figure 8 presents a comparison between the air (Figure 8a) and dew point (Figure 8b) temperatures measured by the Coyote and those obtained from the dropsonde analysis. The temperature comparison (Figure 8a) reveals that the data always agree to within $\pm 2^{\circ}\text{C}$, but the agreement is often much better. In fact, 93% (59%) of the data agree to within $\pm 1^{\circ}\text{C}$ (0.5°C). The mean temperature of both time series is 20.9°C (Table 5), and three individual dropsonde measurements (Table 4; green squares in Figure 8a) lend confidence to both the analysis values and the Coyote measurements. However, a greater discrepancy is present in the dew point temperature comparison (Figure 8b; mean difference of 1.3°C), mostly between 260 km and 195 km from the center. In this region, the Coyote measures dew point temperatures $1\text{--}2.5^{\circ}\text{C}$ greater than the dropsonde analysis indicates. There were three dropsonde measurements within 20 km of the Coyote that were taken during the Coyote flight (Table 4; green squares in Figure 8b). The dropsonde and Coyote measurements made at the same altitudes at radial distances of 238 km and 210 km differ by 1.4°C and 3.3°C , respectively. However, the Coyote measurements reveal that the latter dropsonde was near a sharp radial gradient in moisture (Figure 8b; second green square from left). When the same dropsonde measurement at 210 km is compared to the Coyote measurement at 208.8 km, the measurements differ by only 0.3°C . Since the dropsonde and Coyote measurement locations were 8 km from each other (Table 4), it is conceivable that the radial location of the sharp moisture gradient differed slightly between the two platforms.

The fine-scale variations in temperature and moisture documented by Coyote may offer key insights into TC thermodynamic structure within the poorly observed hurricane boundary layer. Currently, only dropsondes and ocean buoys can be used to retrieve thermodynamic data from these critical areas of the open ocean, and such measurements are rare in both time and space. UAS such as Coyote therefore offers the scientific community a unique opportunity for improved documentation within these data sparse regions.

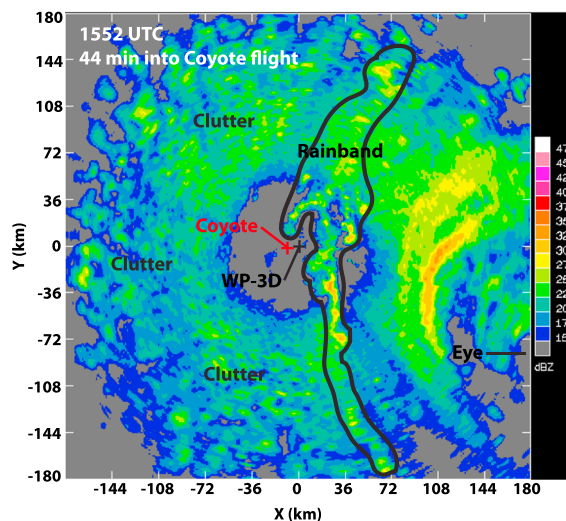


Figure 7. Radar reflectivity observed by the lower fuselage (LF) radar aboard N42RF at 1552 UTC on 17 September 2014. The approximate Coyote and WP-3D positions are indicated by the red and black plus signs, respectively. A rainband from Hurricane Edouard is outlined in black.

5. Summary and Future Work

In this research, we presented Coyote UAS measurements made in the eye, eyewall, and inflow layer of Hurricane Edouard on 16 September 2014 (eye/eyewall) and 17 September 2014 (near-surface inflow layer). These data are the first ever to be collected by a UAS that was released into a TC by a manned aircraft and the first measurements of the meteorological conditions in a TC made by the Coyote platform. To assess the data accuracy, comparisons between the Coyote measurements and those made by NOAA's

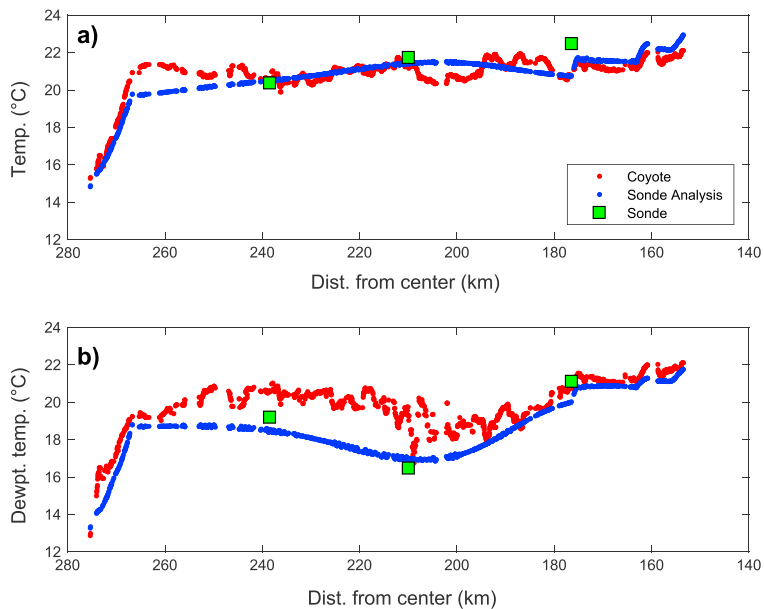


Figure 8. As in Figure 6 but for (a) air temperature and (b) dew point temperature.

WP-3D and GPS dropsondes were presented. Results illustrate that measurements of Coyote UAS winds, atmospheric temperature, and moisture generally compare favorably with observations obtained from the WP-3D and GPS dropsondes.

For the 27-min eye/eyewall flight conducted on 16 September, Coyote observations compared exceptionally well within the light-wind eye environment of Hurricane Edouard. Here winds, temperature, and dew point were found to match up very well with comparable estimates from dropsondes and the WP-3D (Figures 3b, 4a, and 4b). An individual GPS dropsonde was also found to have wind speeds that matched those of the Coyote at their common altitude. Within the ~10 km transition region between the eye and the eyewall, both the Coyote and the WP-3D flight-level wind measurements illustrate a gradual increase in the wind speed, which eventually peaked in the eyewall at 51.5 m s^{-1} (Coyote), 55.6 m s^{-1} (WP-3D inbound leg; adjusted to Coyote altitude), and 59.5 m s^{-1} (WP-3D outbound leg; adjusted to Coyote altitude). Limited temperature and dew point comparisons within the transition and eyewall regions illustrate good overall agreement between individual and composite GPS dropsonde analyses and Coyote measurements.

On 17 September, the Coyote UAS collected data for 68 min at altitudes ranging from 760 to 250 m. This experiment was conducted within a region of the storm that was not dominated by large horizontal gradients and served as a proxy for simulating inflow into a hurricane. This longer-duration mission enabled a more detailed comparison of Hurricane Edouard's winds, temperature, and moisture fields. On 17 September, analyses comparing the Coyote winds with GPS dropsonde-derived analyses of total and radial wind were particularly robust (Figures 6b and 6c). In addition, the mean difference in the Coyote and dropsonde-measured air temperatures was less than 0.1°C (Table 5). While average dew point temperature differences were found to be 1.3°C , it is worth noting that two of the three individual dropsondes closest to the Coyote in time and space exhibited much smaller differences of 0.3°C (when the sharp radial gradient in moisture was considered) and 0.4°C . These results suggest that averaged analyses, while useful in determining a baseline, realistic range for these comparisons, may have limited utility when it comes to accurately assessing the absolute validity of individual in situ observations. It is also worth noting that the average 1.3°C difference in dew point temperature illustrated in Table 5 and shown in Figure 8b represents a Coyote "moist bias" relative to the dropsonde dew point temperature measurements. However, it is currently unclear whether the relatively larger Coyote dew point temperatures are due to an actual moist bias from the InterMet sensors, a previously documented GPS dropsonde dry bias [Vance *et al.*, 2004], an artifact of the composite analysis itself, or a combination of these factors. It is believed that further testing and additional Coyote-dropsonde data comparisons are required to answer this question more completely.

Future work using the Coyote platform will include chamber testing of the InterMet payload to further document sensor performance (and better assess the wet/dry bias question described previously). Additional Coyote UAS in-storm flights are planned for 2016 along with clear-air testing early in 2016. In 2016, Coyote hurricane missions will also utilize a new downward-looking infrared sensor that will be capable of measuring sea surface temperature. This new measurement will expand the Coyote's existing suite of instrumentation that already includes atmospheric pressure, temperature, moisture, and wind speed and direction. Coyote measurements will also be used to compare and validate physical fields simulated by NOAA's coupled Hurricane Weather Research and Forecasting operational modeling system. Observing System Experiments and Observing System Simulation Experiments are planned to optimize observing strategies and quantify the impact that these unique data may have on hurricane intensity forecasts.

Longer-term goals include plans to transform today's Coyote UAS into a hybrid platform that leverages existing GPS dropsonde and Airborne Vertical Atmospheric Profiling System technologies with advanced UAS targeting capabilities. It is possible that a next generation "UASonde" system could be built and tested for future operational applications within the next few years.

Acknowledgments

The Disaster Relief Appropriations Act of 2013 provided funds for the purchase, testing, and operations of the Coyote UAS. Evan Kalina held an NRC Research Associateship award at the Atlantic Oceanographic and Meteorological Laboratory (AOML) and the Earth System Research Laboratory (ESRL) while this research was performed. Special thanks go out to Commander Kristie Twining at NOAA/OMAO for her tireless efforts supporting the project. The authors also wish to thank the NOAA/AOC WP-3D crew members associated with the 16–17 September 2014 flights discussed within this manuscript. Without their professional expertise, successful execution of these landmark UAS missions would not have been possible. Thanks also go out to ItriCorp's Jim Etro and Dave Downer for their help designing, testing, and integrating the meteorological payload used during 2014 operations. The authors would like to acknowledge Raytheon engineers Andrew Osbrink, Chris Trout, and Eric Redweik for their dedication throughout the entire process. Finally, we thank Jun Zhang for his helpful feedback on this manuscript. The data used for these analyses are available at http://www.aoml.noaa.gov/hrd/data_sub/

References

- Black, P. G., E. A. D'Asaro, T. B. Sanford, W. M. Drennan, J. A. Zhang, J. R. French, P. P. Niiler, E. J. Terrill, and E. J. Walsh (2007), Air-sea exchange in hurricanes: Synthesis of observations from the coupled boundary layer air-sea transfer experiment, *Bull. Am. Meteorol. Soc.*, *88*, 357–374, doi:10.1175/MWR-D-14-00339.1.
- Cascella, G., J. J. Cione, E. W. Uhlhorn, and S. J. Majumdar (2008), Inner-core characteristics of Ophelia (2005) and Noel (2007) as revealed by Aerosonde data, paper presented at 28th Conference on Hurricanes and Tropical Meteorology, Am. Meteorol. Soc., Orlando, Fla.
- Cione, J. J., P. Black, and S. Houston (2000), Surface observations in the hurricane environment, *Mon. Weather Rev.*, *128*, 1550–1561, doi:10.1175/1520-0493(2000)128<1550:SOITHE>2.0.CO;2.
- Cione, J. J., et al. (2008), The first successful unmanned aerial system (UAS) mission into a tropical cyclone (Ophelia 2005), paper presented at 12th Conference on Integrated Observing and Assimilation Systems for Atmosphere, Ocean, and Land Surface (IOAS-AOLS), Am. Meteorol. Soc., New Orleans, La.
- Cione, J. J., E. A. Kalina, J. Zhang, and E. Uhlhorn (2013), Observations of air-sea interaction and intensity change in hurricanes, *Mon. Weather Rev.*, *141*, 2368–2382, doi:10.1175/MWR-D-12-00070.1.
- Franklin, J. L., M. L. Black, and K. Valde (2003), GPS dropwindsonde wind profiles in hurricanes and their operational implications, *Weather Forecast.*, *18*, 32–44, doi:10.1175/1520-0434(2003)018<0032:GDWPIH>2.0.CO;2.
- Hock, T. F., and J. L. Franklin (1999), The NCAR GPS dropwindsonde, *Bull. Am. Meteorol. Soc.*, *80*, 407–420, doi:10.1175/1520-0477(1999)080<0407:TNGD>2.0.CO;2.
- Jorgensen, D. F. (1984), Mesoscale and convective-scale characteristics of mature hurricanes. Part I: General observations by research aircraft, *J. Atmos. Sci.*, *41*, 1268–1286, doi:10.1175/1520-0469(1984)041%3C1268:MACSCO%3E2.0.CO;2.
- Lin, P., and C.-S. Lee (2008), The eyewall-penetration reconnaissance observation of Typhoon Longwang (2005) with unmanned aerial vehicle, Aerosonde, *J. Atmos. Oceanic Technol.*, *25*, 15–25, doi:10.1175/2007JTECHA914.1.
- Stewart, S. R. (2014), Tropical cyclone report: Hurricane Edouard, National Hurricane Center, Miami, Fla.
- Uhlhorn, E. W., and P. G. Black (2003), Verification of remotely sensed sea surface winds in hurricanes, *J. Atmos. Oceanic Technol.*, *20*, 99–116, doi:10.1175/1520-0426(2003)020%3C0099:VORSSS%3E2.0.CO;2.
- Uhlhorn, E. W., P. G. Black, J. L. Franklin, M. Goodberlet, J. Carswell, and A. S. Goldstein (2007), Hurricane surface wind measurements from an operational stepped frequency microwave radiometer, *Mon. Weather Rev.*, *135*, 3070–3085, doi:10.1175/MWR3454.1.
- Vance, A. K., J. P. Taylor, T. J. Hewison, and J. Elms (2004), Comparison of in situ humidity data from aircraft, dropsonde, and radiosonde, *J. Atmos. Oceanic Technol.*, *21*, 921–932, doi:10.1175/1520-0426(2004)021%3C0921:COISHD%3E2.0.CO;2.
- Zhang, J. A., P. G. Black, J. R. French, and W. M. Drennan (2008), First direct measurements of enthalpy flux in the hurricane boundary layer: The CBLAST results, *Geophys. Res. Lett.*, *35*, L14813, doi:10.1029/2008GL034374.